








RESEARCH ARTICLE | APRIL 13 2023

Crack healing behavior of 4H-SiC: Effect of dopants

Xiaoshuang Liu ; Yazhe Wang; Xi Zhang; Yunhao Lu ; Rong Wang  ; Deren Yang ; Xiaodong Pi  

 Check for updates

J. Appl. Phys. 133, 145704 (2023)

<https://doi.org/10.1063/5.0140922>





Instruments for Advanced Science

- Knowledge
- Experience
- Expertise

Click to view our product catalogue

Contact Hiden Analytical for further details:

- www.HidenAnalytical.com
- info@hiden.co.uk

Gas Analysis



- dynamic measurement of reaction gas streams
- catalysis and thermal analysis
- molecular beam studies
- dissolved species probes
- fermentation, environmental and ecological studies

Surface Science



- UHV TPD
- SIMS
- end point detection in ion beam etch
- elemental imaging - surface mapping

Plasma Diagnostics



- plasma source characterization
- etch and deposition process reaction kinetic studies
- analysis of neutral and radical species

Vacuum Analysis



- partial pressure measurement and control of process gases
- reactive sputter process control
- vacuum diagnostics
- vacuum coating process monitoring

Crack healing behavior of 4H-SiC: Effect of dopants

Cite as: J. Appl. Phys. 133, 145704 (2023); doi: 10.1063/5.0140922

Submitted: 1 January 2023 · Accepted: 22 March 2023 ·

Published Online: 13 April 2023



Xiaoshuang Liu,^{1,2,3} Yazhe Wang,^{1,2} Xi Zhang,^{1,2} Yunhao Lu,³ Rong Wang,^{1,2,a)} Deren Yang,^{1,2} and Xiaodong Pi^{1,2,a)}

AFFILIATIONS

¹State Key Laboratory of Silicon and Advanced Semiconductor Materials and School of Materials Science and Engineering, Zhejiang University, Hangzhou 310027, China

²Institute of Advanced Semiconductors & Zhejiang Provincial Key Laboratory of Power Semiconductor Materials and Devices, Hangzhou Innovation Center, Zhejiang University, Hangzhou, Zhejiang 311200, China

³Zhejiang Province Key Laboratory of Quantum Technology and Device, Department of Physics, Zhejiang University, Hangzhou 310027, China

^{a)}Authors to whom correspondence should be addressed: rong_wang@zju.edu.cn and xdpi@zju.edu.cn

ABSTRACT

We investigate the crack-healing mechanism of 4H silicon carbide (4H-SiC) and reveal the effect of dopants on the crack-healing behavior of 4H-SiC. Vickers indentation tests and thermal annealing are utilized to generate cracks and heal cracks in 4H-SiC, respectively. High-temperature thermal annealing in the air atmosphere is found to be capable of effectively healing indentation-induced cracks and releasing indentation-induced stress in undoped 4H-SiC by the formation and viscous flow of glass phase SiO₂. Nitrogen (N) doping is found to assist the atomic diffusion of 4H-SiC. The crack healing of N-doped 4H-SiC is realized by the synergy of host solid diffusion and the padding of glassy SiO₂. In contrast, vanadium (V) doping hinders the viscous flow of SiO₂ and results in the incomplete healing of cracks in V-doped 4H-SiC. Although the generation of cracks lowers the bending strength of 4H-SiC, the healing of cracks by the padding of glassy SiO₂ is found to effectively recover the bending strength of indented 4H-SiC samples. Our work opens a pathway to design thermal processing technologies to heal the cracks and enhance the mechanical properties of 4H-SiC wafers.

Published under an exclusive license by AIP Publishing. <https://doi.org/10.1063/5.0140922>

I. INTRODUCTION

4H silicon carbide (4H-SiC) holds great promise in the applications of high-power converters and high-frequency communications, owing to its superior properties including wide bandgap, high breakdown electric field strength, high electron saturation mobility, and strong radiation resistance.^{1–3} After the single-crystal growth of 4H-SiC boules, 4H-SiC substrate wafers are obtained by mechanical processing technologies including wire sawing, grinding, lapping, and chemical-mechanical polishing (CMP).^{4–6} Due to the high brittleness of 4H-SiC, cracks and microcracks are often generated during the mechanical wafering of 4H-SiC substrates,⁷ which lowers the fracture strength, reduces the yield, and, thus, increases the production cost of 4H-SiC wafers.

The most well-developed 4H-SiC substrate wafers are nitrogen (N)-doped, vanadium (V)-doped, and undoped (often referred to as high purity semi-insulating) 4H-SiC wafers.⁸ N-doped 4H-SiC wafers are used as the substrate for the homoepitaxy and applied in

4H-SiC based power devices. The thickness of *n*-type 4H-SiC substrate wafers is 350 μm.⁹ During the device processing of 4H-SiC based power devices, back grinding is frequently used to reduce the thickness of 4H-SiC substrates to 150 μm, which is critical to miniaturizing the device package, reducing the resistance and, thus, power consumption of 4H-SiC based high-power devices.¹⁰ From the point of view of improving the processing efficiency and reducing the cost, it is imperative to directly use thin 4H-SiC substrate wafers of 150 μm for the homoepitaxy and device processing. However, the thin 4H-SiC wafers are susceptible to the formation and extension of cracks and microcracks during the processing of 4H-SiC wafers.^{11,12} Undoped and V-doped 4H-SiC wafers are used as the substrates of the heteroepitaxy of gallium nitrides, during which the formation and healing of cracks are of great importance to the application of 4H-SiC wafers. Therefore, healing the cracks is imperative to the application of 4H-SiC wafers. The concentrations of N and V are in the orders of magnitude of 10¹⁹ and 10¹⁷ cm⁻³, respectively.^{13,14} Understanding the effect of dopants on the crack

11 April 2024 12:30:11

healing behaviors of 4H-SiC is critical to optimize the processing technologies and increase the yield of 4H-SiC wafers.¹⁵

In this work, we investigate the mechanism of the crack healing of 4H-SiC and reveal the effect of dopants on the crack-healing behavior of 4H-SiC. Vickers indentation tests and thermal annealing are utilized to generate and heal cracks in 4H-SiC, respectively. By combining high-temperature thermal annealing, Raman spectra, and transmission electron microscope (TEM) observations, we find that high-temperature thermal annealing in the air atmosphere is capable of effectively releasing the indentation-induced stress, and healing indentation-induced cracks in undoped 4H-SiC by the formation and viscous flow of the glass phase SiO₂. N doping is found to promote the atomic diffusion of 4H-SiC, and the crack healing of 4H-SiC is realized by the synergy of host solid diffusion and padding of SiO₂. In contrast, V doping hinders the viscous flow of SiO₂ and results in the incomplete healing of cracks in V-doped 4H-SiC. Although the generation of cracks lowers the bending strength of 4H-SiC, the healing of cracks by the viscous flow of SiO₂ is found to effectively recover the bending strength of indented 4H-SiC samples.

II. EXPERIMENTAL METHODS

Undoped, N-doped, and V-doped 4H-SiC single-crystal boules were grown by the physical-vapor-transport (PVT) approach. The concentrations of V and N are in the order of magnitude 10¹⁷ and 10¹⁹ cm⁻³, respectively. 4H-SiC wafers were obtained by slurry-wire sawing, grinding, lapping, and CMP. The surface roughness of all samples is smaller than 0.2 nm. 4H-SiC wafers were cut into 10 × 10 mm² samples. Vickers indentation (MTS, Nano Indenter

XP) tests were carried out in the center of the samples with a load of 9.8 N in air. The healing of cracks was achieved by annealing the indented 4H-SiC samples in an air atmosphere under temperatures ranging from 1473 to 1873 K and durations ranging from 20 min to 10 h.

The surface profiles of 4H-SiC samples before and after thermal annealing were collected using a scanning electron microscope (SEM) (Carl Zeiss, Gemini300) and a three-dimensional optical profilometer (Bruke, ContourX-200). The residual stress was identified by Raman spectroscopy (LabRAM Odyssey, Horiba) excited by a 100 mW, 532 nm laser. The cross-sectional transmission electron microscopy (TEM) specimens of indent imprints were fabricated by the focused ion beam (FIB) technique using a FEI, Helios 5 UX FIB. TEM analysis was then performed using an FEI Tecnai G² field emission transmission electron microscope operating at 200 kV to characterize the microstructures of the cross-sectional morphologies of the 4H-SiC samples. The bending test of a crack-healed specimen was carried out at room temperature to 1273 K. All the bending tests were performed on the stage of a three-point bending-test system with a 16 mm bending span (the crosshead speed is 0.5 mm/min) at room temperature and elevated temperatures. The samples were heated to a testing temperature at a rate of 10 °C/min and soaked for 20 min before testing.¹⁶

III. RESULTS AND DISCUSSION

Figure 1 shows the SEM images of indent imprints in undoped 4H-SiC before and after crack healing at various temperatures. As shown in Fig. 1(a), the length of cracks is approximately 50 μm after indentation. Material removal due to the propagation

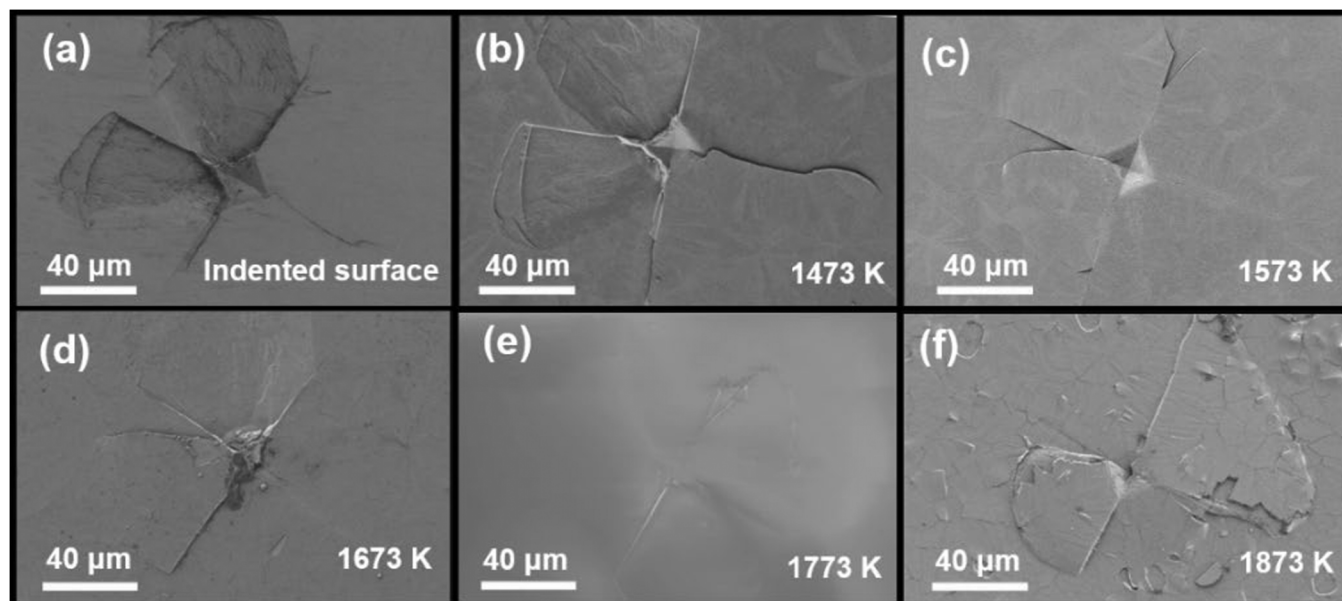


FIG. 1. SEM images of (a) an indent imprint after indentation and [(b)–(e)] indent imprints after thermal annealing for 1 h at different temperatures of undoped 4H-SiC. The annealing temperatures are labeled in each figure.

11 April 2024 12:30:11

of cracks is observed around the indentation. The healing of cracks is observed after thermal annealing of the indented 4H-SiC samples with the annealing duration of 1 h. As the annealing temperature increases from 1473 to 1773 K, the surface of the indented 4H-SiC gradually becomes smooth and the indent imprint and cracks can be faintly seen. This indicates that the indent imprint and cracks are healed by high-temperature annealing at the air atmosphere [Figs. 1(b)–1(d)]. Under the annealing temperature of 1773 K, the indent imprint and cracks are invisible, indicating that they are completely healed [Fig. 1(d)]. When the annealing temperature is as high as 1873 K, pits and bulges are found at the surface of indented 4H-SiC [Fig. 1(e)]. The effect of the annealing duration on the crack-healing behaviors of indented 4H-SiC is then evaluated. As shown in Fig. S1 in the [supplementary material](#) for the indented 4H-SiC sample healed at 1773 K, the optimal annealing duration is 1 h. Therefore, we use the annealing temperature of 1773 K and annealing duration of 1 h to investigate the crack-healing mechanism and the effect of dopants on the crack healing of 4H-SiC.

In order to clarify the mechanism of the healing of indent imprints and cracks by high-temperature annealing, we investigate the micro-Raman spectroscopy of the center of the indent imprint before and after crack-healing treatment. As shown in Fig. 2(a), the Raman spectra of the indent imprint exhibit three characteristic peaks located at 204, 776, and 964 cm^{-1} , which are attributed to the first order of the folded modes of the transverse acoustic branch (FTA), transverse optical branch (FTO), and the longitudinal optical branch (FLO) of 4H-SiC, respectively.^{13,17} Two weak peaks locating at 1524 and 1713 cm^{-1} representing the second-order Raman scattering of 4H-SiC are also observed.⁹ After the thermal annealing at 1773 K for 1 h, the Raman peak located at 490 cm^{-1} is observed at the center of the indent imprint, which is the characteristic peak of amorphous SiO_2 .^{18–20} This suggests that the crack healing is achieved by the oxidation of undoped 4H-SiC under an air atmosphere. In addition, the crack healing reaction of the specimen is estimated as $\text{SiC(s)} + \frac{3}{2}\text{O}_2\text{(s)} = \text{SiO}_2\text{(l)} + \text{CO(g)}$. Furthermore, the broadening of the FTA peak indicates the degradation of the 4H-SiC crystalline character. The peak-intensity mappings of the characterized peaks of amorphous SiO_2 (490 cm^{-1}) and 4H-SiC (204 cm^{-1}) are then carried out to verify the crack-healing mechanism of undoped 4H-SiC. As shown in Figs. 2(b) and 2(c), the peak intensity of 490 cm^{-1} inside the indent imprint is much higher than that of the pristine surface, while the peak intensity of 204 cm^{-1} inside the indent imprint is much lower than that of the pristine surface. This indicates that the padding of amorphous SiO_2 is more involved in the crack healing of 4H-SiC than the solid diffusion of 4H-SiC. We note that the Raman spectra of the 4H-SiC surface after crack healing have two broadened peaks located at 1330 and 1618 cm^{-1} , which are attributed to the graphitization of the surface due to silicon overflow during crack healing.²¹

During crack healing, the padding of amorphous SiO_2 might be affected by the residual stress induced by indentation. We then employ the micro-Raman peak mapping of the FTO mode, which is associated with the residual stress of 4H-SiC, to characterize the distribution of the residual stress of indented 4H-SiC before and after crack healing. The positive and negative shifts of the peak of the FTO mode indicate the compressive stress and tensile residual

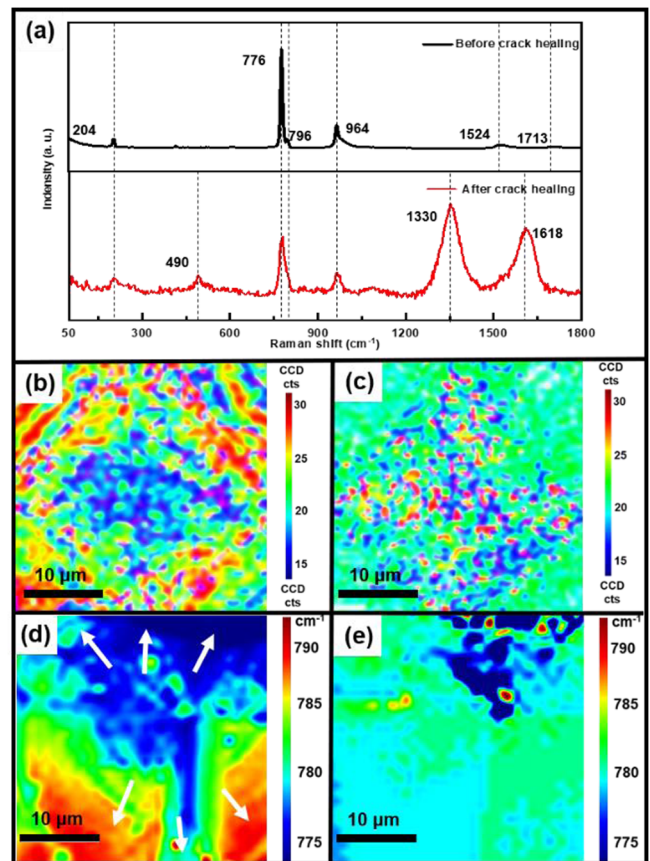


FIG. 2. (a) Micro-Raman spectra obtained at the center of indent imprints of undoped 4H-SiC before and after crack healing at 1773 K. Micro-Raman intensity mapping of the peaks locating at (b) 204 and (c) 490 cm^{-1} of the indent imprints on the surface of undoped 4H-SiC. Peaking-position mapping of the FTO mode of the cross-sectional indent imprint of 4H-SiC (d) before and (e) after crack healing. The white arrows in (c) point to the direction of the residual stress in undoped 4H-SiC after indentation.

stress, respectively.^{22–24} For undoped 4H-SiC after indentation, the FTO peak shifts to lower wavelength numbers at the subsurface of the indent imprint, indicating that there exists tensile stress after indentation [Fig. 2(d)]. The deeper region below the indent imprint has compressive stress, evidenced by the higher wavelength numbers of the FTO peak in this region [Fig. 2(d)]. After crack healing, the compressive stress under the indent imprint is released, as evidenced by the uniform distribution of the FTO peak position [Fig. 2(e)]. This indicates that the release of residual stress is accompanied by crack healing. The activation of the padding of amorphous SiO_2 needs to overcome the energy barrier to make one molecule transition from one particular state to another.²⁵ In the case of crack healing of 4H-SiC, the activation of viscous flow mainly originates from the gravity of glass phase SiO_2 . The peaking-position Raman mapping suggested that the direction of internal stress is opposite to the direction of the gravity components, which hinders the viscous flow of glass phase SiO_2 .^{26–28}

11 April 2024 12:30:11

The effect of dopants on the crack healing of 4H-SiC is then evaluated by investigating the change in the indentation depths of differently doped 4H-SiC before and after thermal annealing. As shown in Figs. 3(a) and 3(b), the indent imprints of undoped

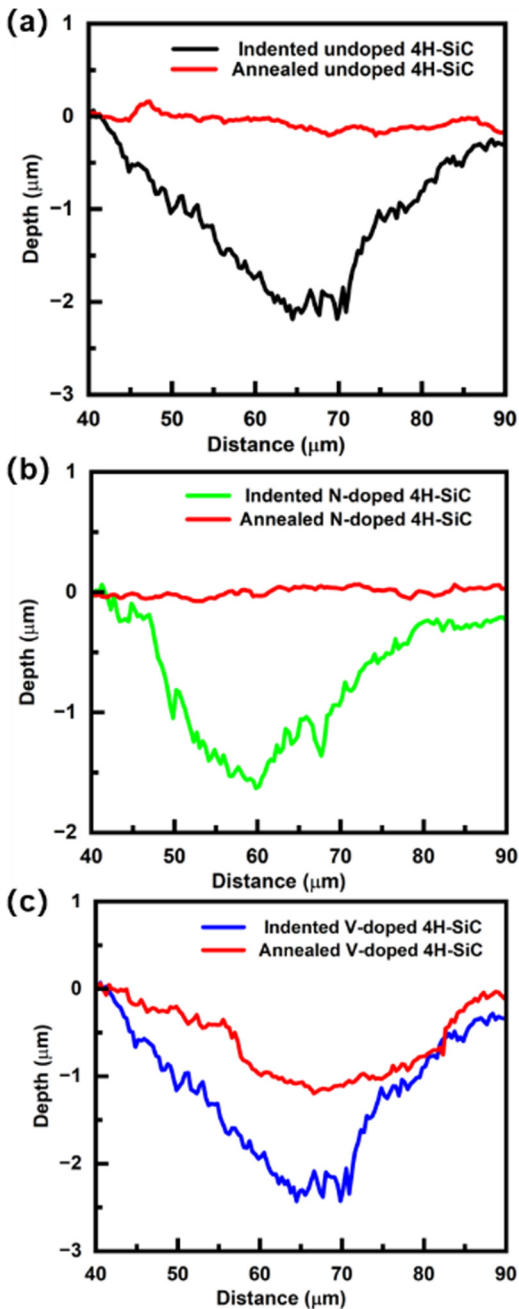


FIG. 3. The indentation depth taken along the diagonal direction before and after crack healing at 1773 K of indent imprints of (a) undoped, (b) N-doped, and (c) V-doped 4H-SiC.

4H-SiC and N-doped 4H-SiC are completely healed after thermal annealing at 1773 K for 1h. In contrast, the maximum residual depth of the indent imprint of V-doped 4H-SiC decreases from 2.38 to 1.19 μm after thermal annealing, indicating that the indent imprint of V-doped 4H-SiC is not completely healed [Fig. 3(c)]. Meanwhile, we find that the maximum residual depth of the indent imprints decreases in the order of V-doped, undoped, and N-doped 4H-SiC, as a result of decreased hardness and brittleness.¹⁷

The recovery ratio (δ) of the indented 4H-SiC is calculated by¹³

$$\delta = \frac{(h_0 - h_a)}{h_0}, \quad (1)$$

where h_0 and h_a are the maximum residual depths of the indent imprint before and after thermal annealing, respectively. The calculated recovery ratios of undoped, N-doped, and V-doped 4H-SiC are 1, 1, and 0.5, respectively.

The cross-sectional microstructure and elemental distribution of the filled indent imprints of differently doped 4H-SiC are investigated by TEM and EDX to reveal the effect of dopants on the crack healing mechanism of 4H-SiC. As shown in Fig. 4(a), the indent imprint of undoped 4H-SiC has been completely healed after thermal annealing. The distribution of the C element verifies that the indent imprint and lateral cracks are formed after indentation.²⁴ The distributions of Si and O are found in the filled cracks and the indent imprint, while C almost disappears in the crack filling of undoped 4H-SiC. This indicates that the padding of amorphous oxides is involved in the crack healing of undoped 4H-SiC. For N-doped 4H-SiC, the EDX mappings of C, Si, and O elements are found in the filled cracks and indent imprint [Fig. 4(b)]. This suggests that both the padding of amorphous oxides and the solid diffusion of 4H-SiC participate in the crack healing of N-doped 4H-SiC. The solid diffusion is considered to be hardly occurred in undoped 4H-SiC due to the low diffusion coefficients and high activation energies of both Si and C atoms.^{29–31} N dopants have been found to be capable of assisting the long-range transport of Si atoms in SiC.²⁷ The activation energies of atomic diffusion in undoped 4H-SiC and N-doped 4H-SiC are -7.41 ± 0.05 and -8.20 ± 0.08 eV/atom, respectively.^{30,32} This explains why the healing of N-doped 4H-SiC also originates from solid diffusion. Since the elemental distribution of O is more obvious than that of C, the effect of the padding of amorphous oxides prevails over the effect of solid diffusion. We note that voids are found in the healed cracks in N-doped 4H-SiC, indicating the incomplete healing of cracks at the center of cracks due to the incomplete dense of oxides. For V-doped 4H-SiC, the surface of the indent imprint is covered by a SiO₂ layer, and the solid diffusion of host atoms is not found in V-doped 4H-SiC [Fig. 4(c)]. This indicates that the healing of cracks in V-doped 4H-SiC is achieved by the padding of amorphous SiO₂. V doping is found to decrease the fracture toughness of 4H-SiC and accumulate high residual stress upon indentation,^{19,31} which hinders the padding of amorphous SiO₂, thus resulting in the fact that the indent imprint is not completely healed after thermal annealing.

11 April 2024 12:30:11

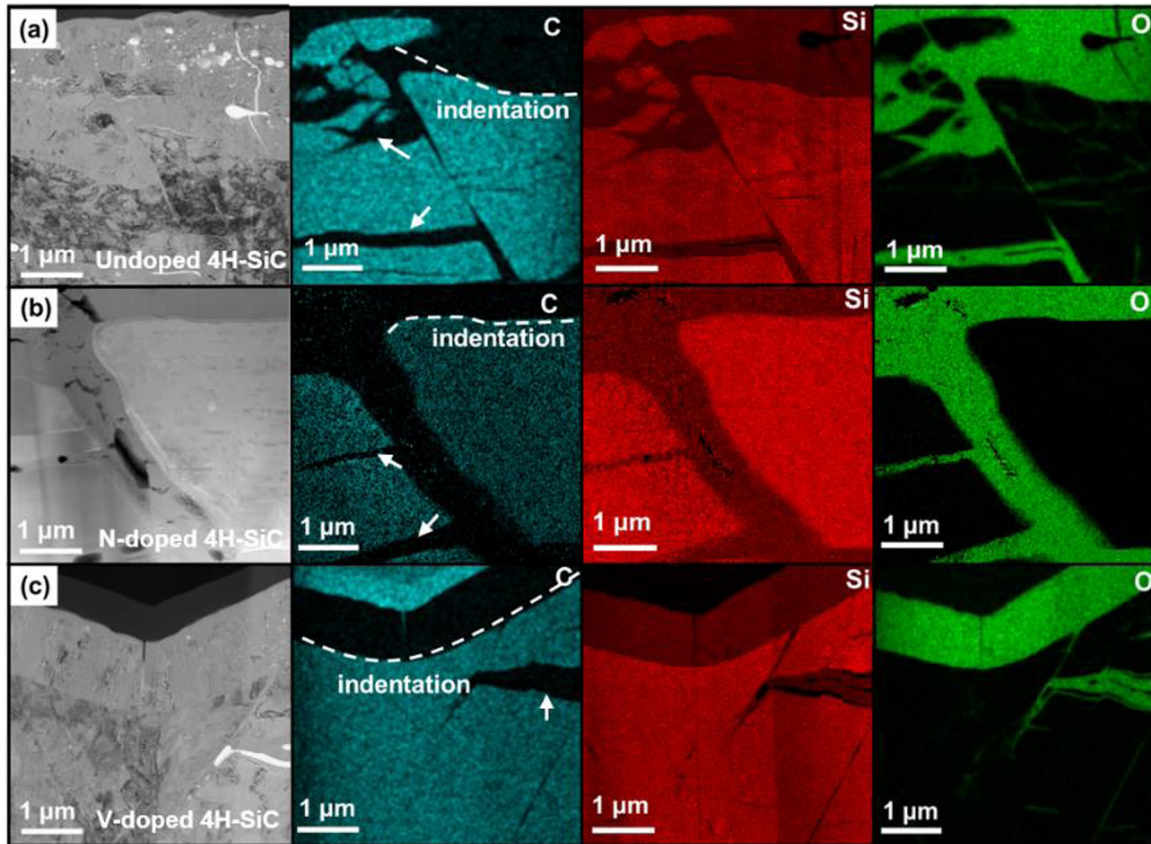


FIG. 4. Cross-sectional TEM images and the corresponding EDX mapping micrographs of C, Si, and O elements of (a) undoped, (b) N-doped, and (c) V-doped 4H-SiC after crack healing at 1773 K. The white arrow in the EDX mapping micrographs of C elements indicates the lateral cracks.

11 April 2024 12:30:11

Since we reveal that the cracks in 4H-SiC can be healed by thermal annealing, we then evaluate whether the mechanical properties of 4H-SiC can be recovered after thermal annealing. The bending strengths of the differently doped indented 4H-SiC samples as functions of the crack-healing temperature are shown in Fig. 5(a). It is clear that the bending strength of differently doped 4H-SiC gradually increases with the increase in the crack-healing temperature, indicating that the bending strength can be recovered by the healing of cracks. However, when the annealing temperature is higher than 1773 K, the bending strength decreases dramatically, which is ascribed to the material loss through the formation of volatile species (SiO and CO). More significantly, the bending strength of undoped 4H-SiC and N-doped 4H-SiC recovers up to 572 and 584 MPa, respectively, which are consistent with the bending strength of 4H-SiC at room temperature.³³ This indicates that the mechanical properties of undoped and N-doped 4H-SiC can be completely recovered after crack healing. For V-doped 4H-SiC, the bending strength is partially recovered due to the incomplete crack healing. We have also investigated the effect of the crack length on the bending strength of 4H-SiC to determine the critical crack size. As shown in Fig. S2 in the [supplementary](#)

[material](#), the bending strength of crack-healed 4H-SiC dramatically decreases when the crack length is higher than 450 μm . Therefore, the critical crack size for undoped 4H-SiC is 450 μm . When the crack size is higher than 450 μm , the crack cannot be healed by thermal annealing at 1773 K, 1 h.

The effect of dopants on the bending strength originates from the different crack healing mechanisms in differently doped 4H-SiC. N doping is found to increase the bending strength of 4H-SiC with the assistance of the solid diffusion of 4H-SiC. In contrast, V doping increases the residual stress of Vickers indentation, which hinders the SiO₂ glass viscous flow and results in the lower bending strength of V-doped 4H-SiC. Due to the high integration of 4H-SiC devices, the operating temperature for 4H-SiC devices is usually high. The stable operating temperature of 4H-SiC devices reaches 800 K. Figure 5(b) shows the effect of the bending-test temperature on the bending strength of the differently doped 4H-SiC after thermal annealing at 1773 K for 1 h. The bending strength for undoped 4H-SiC keeps a high value (~ 580 MPa) of up to 873 K. Over 873 K, the bending strength decreases suddenly and exhibited a low value of ~ 300 MPa as a result of the softening of the glass phase SiO₂ at high

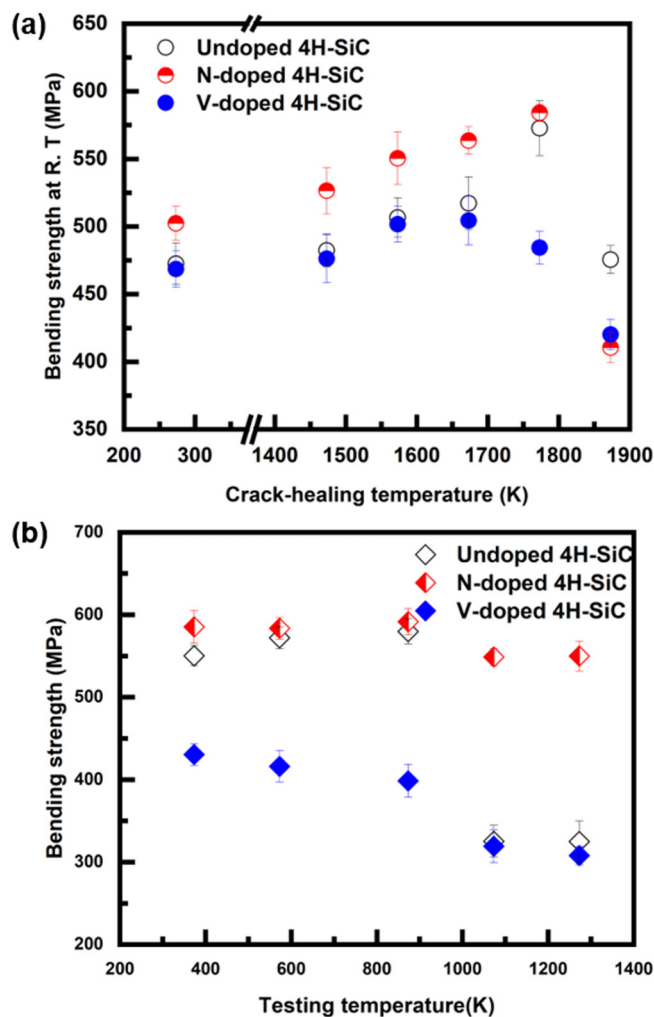


FIG. 5. Dependence of the bending strength on the (a) crack-healing temperature and (b) testing temperature of differently doped 4H-SiC. The bending strength is the average value of the bending strength for the five measured values, with error bars connecting the maximum and the minimum values.

temperature.³¹ In contrast, the bending strength for N-doped 4H-SiC holds a steady value of ~ 540 MPa. As mentioned earlier, the solid diffusion of Si and C atoms played a partial role in the crack healing of N-doped 4H-SiC. The re-sintering 4H-SiC can maintain a relatively high strength under the high test temperature. However, the bending strength for V-doped 4H-SiC remains at a relatively low value of ~ 300 MPa after crack healing, resulting from the incomplete crack healing of V-doped 4H-SiC.

IV. CONCLUSIONS

In conclusion, we have systematically investigated the crack-healing mechanism and the effect of dopants on the crack-healing mechanism of 4H-SiC. Vickers indentations and cracks of undoped

4H-SiC are completely healed by thermal annealing at 1773 K for 1 h in the air atmosphere. The crack-healing mechanism of undoped 4H-SiC has been confirmed to be the oxidation-induced crack healing and solid diffusion, in which the former is achieved by the viscous flow of the glass phase SiO_2 and the volume expansion from SiC to SiO_2 . N doping is found to assist the solid diffusion of 4H-SiC to fill cracks by promoting the self-diffusion of 4H-SiC, which result in the high bending strength of N-doped 4H-SiC at high temperature. In contrast, V doping hinders the SiO_2 glass viscous flow due to the residual stress of Vickers indentation and results in the incomplete crack healing of V-doped 4H-SiC. Our work indicates that the mechanical processing induced cracks and microcracks can be healed by high-temperature thermal annealing in the air atmosphere, which recovers the mechanical properties of 4H-SiC wafers.

SUPPLEMENTARY MATERIAL

See the [supplementary material](#) for the SEM images of the indent imprints after thermal annealing at different temperatures in undoped 4H-SiC.

ACKNOWLEDGMENTS

This work was supported by the National Natural Science Foundation of China (Grant Nos. 62204216, 62274143, and U22A2075), the “Pioneer” and “Leading Goose” R&D Program of Zhejiang (Grant Nos. 2022C01021 and 2023C01010), the Leading Innovative and Entrepreneur Team Introduction Program of Hangzhou (No. TD2022012), the Natural Science Foundation of China for Innovative Research Groups (Grant No. 61721005), and the Zhejiang University Education Foundation Global Partnership Fund.

AUTHOR DECLARATIONS

Conflict of Interest

The authors have no conflicts to disclose.

Author Contributions

Xiaoshuang Liu: Data curation (equal); Formal analysis (equal); Investigation (equal); Writing – original draft (equal). **Yazhe Wang:** Formal analysis (equal); Investigation (equal); Methodology (equal). **Xi Zhang:** Formal analysis (equal); Investigation (equal); Writing – review & editing (equal). **Yunhao Lu:** Conceptualization (equal); Visualization (equal); Writing – review & editing (equal). **Rong Wang:** Data curation (equal); Investigation (equal); Writing – review & editing (equal). **Deren Yang:** Funding acquisition (equal); Writing – review & editing (equal). **Xiaodong Pi:** Funding acquisition (equal); Visualization (equal); Writing – review & editing (equal).

DATA AVAILABILITY

The data that support the findings of this study are available from the corresponding authors upon reasonable request.

REFERENCES

- ¹T. Kimoto and J. A. Cooper, *Fundamentals of Silicon Carbide Technology: Growth, Characterization, Devices and Applications* (Wiley, 2014), p. 353.
- ²A. Bedoya-Pinto, J. R. Ji, A. K. Pandeya, P. Gargiani, M. Valvidares, P. Sessi, J. M. Taylor, F. Radu, K. Chang, and S. S. Parkin, *Science* **374**, 616 (2021).
- ³M. Omidian, S. Leitherer, N. Neel, M. Brandbyge, and J. Kroeger, *Phys. Rev. Lett.* **126**, 216801 (2021).
- ⁴S. Dogan, D. Johnstone, F. Yun, S. Sabuktagin, J. Leach, A. A. Baski, H. Morkoc, G. Li, and B. Ganguly, *Appl. Phys. Lett.* **85**, 1547 (2004).
- ⁵M. Losurdo, G. Bruno, A. Brown, and T. H. Kim, *Appl. Phys. Lett.* **84**, 4011 (2004).
- ⁶C. Yao, D. Chen, K. Xu, Z. Zheng, Q. Wang, and Y. Liu, *Mater. Sci. Semicond. Process.* **123**, 105512 (2021).
- ⁷Z. Zhang, Z. D. Wen, H. Y. Shi, Q. Song, Z. Y. Xu, M. Li, Y. Hou, and Z. C. Zhang, *Micromachines* **12**, 1331 (2021).
- ⁸J. J. Li, H. Luo, G. Yang, Y. Q. Zhang, X. D. Pi, D. R. Yang, and R. Wang, *Phys. Rev. Appl.* **17**, 054011 (2022).
- ⁹R. Rupp, R. Gerlach, U. Kichner, A. Schlogl, and R. Kem, *Mater. Sci. Forum* **717**, 921 (2012).
- ¹⁰K. Masumoto, S. Segawa, T. Ohno, S. Tsukimoto, K. Kojima, T. Kato, and H. Okumura, *Jpn. J. Appl. Phys.* **58**, SBBD10 (2019).
- ¹¹X. S. Liu, R. Wang, J. R. Wang, Y. H. Lu, Y. Q. Zhang, D. R. Yang, and X. D. Pi, *J. Phys. D: Appl. Phys.* **55**, 494001 (2022).
- ¹²H. Jacobson, J. Birch, C. Hallin, A. Henry, R. Yakimova, T. Tuomi, E. Janzen, and U. Lindefelt, *Appl. Phys. Lett.* **82**, 3689 (2003).
- ¹³M. K. Linnarsson, A. Hallen, and L. Vines, *Semicond. Sci. Technol.* **34**, 115006 (2019).
- ¹⁴F. Fujie, S. Harada, K. Hanada, H. Suo, H. Koizumi, T. Kato, M. Tagawa, and T. Ujihara, *Acta Mater.* **194**, 387 (2020).
- ¹⁵X. Geng, F. Yang, Y. Chen, X. Lu, X. Zhong, and P. Xiao, *Acta Mater.* **105**, 121 (2016).
- ¹⁶Y. Sun, W. Lan, T. Zhao, J. Zhao, D. Wu, X. Ma, and D. Yang, *J. Appl. Phys.* **128**, 235105 (2020).
- ¹⁷X. Liu, J. Zhang, B. Xu, Y. Lu, Y. Zhang, R. Wang, D. Yang, and X. Pi, *Appl. Phys. Lett.* **120**, 052105 (2022).
- ¹⁸S. Degioanni, A. M. Jurdyc, A. Cheap, B. Champagnon, F. Bessueille, J. Coulm, L. Bois, and D. Vouagner, *J. Appl. Phys.* **118**, 153103 (2015).
- ¹⁹J. P. Zhao, D. X. Huang, Z. Y. Chen, W. K. Chu, B. Makarenkov, A. J. Jacobson, B. Bahrim, and J. W. Rabalais, *J. Appl. Phys.* **103**, 124304 (2008).
- ²⁰M. Grimsditch, *Phys. Rev. Lett.* **52**, 2379 (1984).
- ²¹A. C. Ferrari and J. Robertson, *Philos. Trans. R. Soc. A* **362**, 2269 (2004).
- ²²M. Yamaguchi, M. Fujitsuka, S. Ueno, I. Miura, W. Erikawa, and T. Tomita, *Mater. Sci. Forum* **645–648**, 551 (2010).
- ²³J. R. Zhang, T. Liang, Y. H. Lu, B. J. Xu, T. Q. Deng, Y. Q. Zhang, Z. D. Zeng, X. D. Pi, D. R. Yang, and R. Wang, *New J. Phys.* **24**, 113015 (2022).
- ²⁴J. Yan, X. Gai, and H. Harada, *J. Nanosci. Nanotechnol.* **10**, 7808 (2010).
- ²⁵Y. Liu, F. P. Van der Meer, L. J. Sluys, and J. T. Fan, *Compos. Struct.* **252**, 112690 (2020).
- ²⁶S. F. Ali and J. T. Fan, *Int. J. Appl. Mech.* **13**, 2150104 (2021).
- ²⁷S. Fateh Ali and J. Fan, *J. Mater. Sci. Technol.* **57**, 12 (2020).
- ²⁸M. H. Hon and R. F. Davis, *J. Mater. Sci.* **14**, 2411 (1979).
- ²⁹M. H. Hon, R. F. Davis, and D. E. Newbury, *J. Mater. Sci.* **15**, 2073 (1980).
- ³⁰J. D. Hong, R. F. Davis, and D. E. Nerbury, *J. Mater. Sci.* **16**, 2485 (1981).
- ³¹X. S. Liu, R. Wang, J. R. Zhang, Y. H. Lu, Y. Q. Zhang, D. R. Yang, and X. D. Pi, *J. Phys. D: Appl. Phys.* **55**, 334002 (2022).
- ³²J. D. Hong and R. F. Davis, *J. Am. Ceram. Soc.* **63**, 546 (1980).
- ³³J. Korous, M. C. Chu, M. Nakatani, and K. Ando, *J. Am. Ceram. Soc.* **83**, 2788 (2000).